MAJOR ARTICLE

TAPROBANICA, ISSN 1800–427X. Vol. 14, No. 02 (2025): pp. 245–259, pl. 25–27. Published by Research Center for Climate Change & Faculty of Mathematics & Natural Sciences, Universitas Indonesia, Depok 16424, INDONESIA.
© distributed under Creative Commons CC-BY 4.0 http://www.taprobanica.org https://doi.org/10.47605/tapro.v14i2.377



OPEN ACCESS

urn:lsid:zoobank.org:pub:D09F7A84-2BCA-4DEA-BD67-11F0455935D0

TWO NEW SPECIES OF THE *Hylarana signata* COMPLEX (ANURA: RANIDAE) FROM SUMATRA AND THE DISTRIBUTION OF *H. sundabarat* (CHAN, ABRAHAM, GRISMER & BROWN, 2020)

Submitted: 19 July 2025, Accepted: 21 October 2025, Published: 25 November 2025 Subject Editor: Koshiro Eto

Amat Ribut^{1*}, Misbahul Munir^{2,5}, A.A. Thasun Amarasinghe², Danny Gunalen³, Eric N. Smith⁴, Achmad Farajallah^{1*} & Amir Hamidy²

Abstract

The *Hylarana signata* complex is species-rich in Indonesia but remains taxonomically unresolved, particularly across Sumatra, where morphological conservatism obscures lineage boundaries. We analyzed Sumatran populations using an integrative dataset comprising adult-male morphology (32 characters) and mitochondrial DNA (16S rRNA, 444 bp). Phylogenetic analyses using Bayesian inference, maximum-likelihood, and neighbour-joining methods revealed two distinct and well-supported lineages, here described as new species. The uncorrected p-distance between them (4.81%) exceeds typical species-level thresholds in anurans. Multivariate analyses (PCA) show partial morphometric overlap with congeners, but the new species are diagnosable by consistent combinations of external traits—including humeral gland size and placement, dorsolateral stripe pattern, and webbing formula—corroborated by mitochondrial divergence. We also confirm *H. sundabarat* in multiple Sumatran provinces, refining its known range in Sundaland. All localities were georeferenced and verified with voucher specimens or genetic data following GBIF citation standards. These findings clarify the composition of the *H. signata* complex in Sumatra and highlight the island's cryptic amphibian endemism and the importance of protected montane forests for biodiversity conservation.

Keywords: Integrative taxonomy, Mitochondrial 16S rRNA, Phylogenetics, Pulchrana, Sumatra

¹ Animal Bioscience, Biology Department, Faculty of Mathematics & Natural Science, IPB University. Kampus IPB Dramaga, Bogor 16680, Indonesia

² Laboratory of Herpetology, Museum Zoologicum Bogoriense, Research Center for Biosystematics & Evolution, National Research & Innovation Agency (BRIN), Cibinong, Indonesia

³ Faunaland Ancol, Ecovention Building - Ecopark, Jl. Lodan Raya, Ancol, Jakarta Utara 14430, Indonesia

⁴Department of Biology, University of Texas at Arlington, Arlington, Texas 76019, USA

⁵ Deceased on 28 February 2023

^{*}Corresponding authors.E-mail: ributamat@gmail.com; achamad@apps.ipb.ac.id

Introduction

Hylarana sensu lato represents a ranid genus that diverged between 30-40 mya (Portik et al. 2023), currently including approximately 103 species distributed across South and Southeast Asia into Australasia (Frost 2025). Indonesia is a hotspot of Hylarana diversity, with roughly 35% of all recognized species and more than half of the Southeast Asian assemblage (36 of 69 species) occurring there (Frost 2025). Indonesian members include H. signata, H. picturata, H. centropeninsularis, H. fantastica, H. siberu, and H. sundabarat. The long and sometimes unstable nomenclatural history of this group began with (i) Polypedates signatus Günther, 1872, from Matang, Sarawak, later transferred through Rana to Hylarana, and (ii) Rana (Hylorana) picturata Boulenger, 1920, from a mixed Bornean syntype series subsequently stabilized by lectotype selection from Mt. Kinabalu (Brown & Guttman 2002). These type-anchored histories highlight taxonomic challenges underlying geographically separated Sundaic populations and underscore the need for an integrative reevaluation.

According to Chan et al. (2014) and Arifin et al. (2018), the above taxa form part of a broader H. signata complex that also includes species from Peninsular Malaysia, Thailand, and the Philippines. Previous work combined morphology, morphometrics, protein electrophoresis, bioacoustics, and DNA sequence data to analyze this complex in Borneo, Peninsular Malaysia, and the Philippines (Brown & Guttman 2002, Zainudin & Sazali 2012, Chan et al. 2020a,b), but comprehensive sampling in Indonesia, particularly Sumatra, has lagged. Sumatra exhibits exceptionally high levels of endemism (Kurniati & Mujiono 2020, Arifin 2024). Arifin et al. (2018) addressed part of this gap by describing H. fantastica from Sumatra and extending the known range of H. centropeninsularis, building on Chan et al. (2014), who highlighted additional undescribed lineages from the island. Notably, *H. sundabarat* was initially reported only from Peninsular Malaysia and southern Thailand, with evidence limited to morphometrics and acoustics and lacking genetic confirmation (Chan et al. 2020a). Although a single Sumatran specimen appeared in a genome-scale gene-flow study (Chan et al. 2020b), broader molecular sampling from Sumatra has been absent. Given the external similarity among Sumatran frogs traditionally identified as H. signata or H. picturata, and the

diagnostic features of Н. sundabarat, misidentifications are likely, implying that H. sundabarat may be more widespread in Sumatra than recognized. Because the nominal concepts of H. signata (Matang, Sarawak) and H. picturata (Bidi Caves, Mt. Kinabalu, and southeastern Borneo; lectotype Mt. Kinabalu) are anchored in Borneo, Sumatran "signata/picturatalike" populations require careful evaluation against type-based diagnoses and modern genetic data (Brown & Guttman 2002; see also Günther 1872, Boulenger 1920). This study aims to clarify the taxonomic status of Sumatran populations within the *H. signata* complex and to update the distribution of H. sundabarat based material deposited at the Museum Zoologicum Bogoriense, Indonesia (MZB). Specifically, we examine series labeled H. Н. Н. picturata, signata, siberu, fantastica, centropeninsularis, Н. and Н. using an integrative sundabarat comprising adult-male external morphology (32 morphometric and qualitative characters) and mitochondrial 16S rRNA sequences. We also include comparative material from Borneo and Peninsular Malaysia to ensure type-consistent interpretation. By situating our evidence within both the historical literature and recent regional syntheses, we refine the composition of the H. signata complex in Sumatra and provide a genetics-anchored distributional update for H. sundabarat, contributing to clearer understanding of amphibian diversity endemism in Indonesia.

Materials and methods

Terminology and data availability. Morphological terminology follows Matsui subsequent (1984)and regional works. Nomenclature follows Frost (2025). The genus assignment follows Hylarana sensu lato after Frost (2025), pending wider resolution of the Pulchrana complex (Chan et al. 2020a). Sequence alignments and matrices are provided as Supplementary Files; new sequences will be uploaded to GenBank upon acceptance, and accession numbers will be added to Sup. Table 1 when issued.

Sampling. Specimens were fixed in 10% buffered formalin and transferred to 70% ethanol for long-term storage. Tissue samples were preserved in lysis buffer (NaCl, EDTA, Tris-Cl, SDS) and frozen. Voucher specimens and tissue samples are deposited in the Museum Zoologicum Bogoriense (MZB) and the

Amphibian and Reptile Diversity Research Center, University of Texas at Arlington (UTA), USA. Newly generated sequences from this study are indicated as "this study" (accessions pending at the time of submission).

Morphological analysis. We focused on adult males to avoid sexual-dimorphism bias. Adult male status was assessed by the presence of humeral glands and/or subgular vocal sacs. When the right side was damaged, homologous measurements were taken on the left side and noted; otherwise, all measurements were taken on the right side. Each metric was measured twice independently with a digital caliper (0.01 mm precision); if the two readings differed by >2%, a third reading was taken and the median recorded. Thirty-two linear characters, largely following Matsui (1984), were recorded: 1) Snout vent length (SVL), distance from the tip of snout to vent; 2) Head length (HL), distance from posterior margin of lower jaw to tip of snout; 3) Head width (HW), distance taken immediately from posterior to eyes; 4) Snout length (SL), distance from anterior corner of the eye to tip of snout; 5) Snout-nostril distance (SNL), distance from tip of the snout to the anterior of nostril; 6) Nostril-eyelid distance (NEL), distance from the posterior edge of the nostril to the anterior edge of the eye; 7); Internarial distance (IND), shortest distance between the inner margins of the nostrils; 8) Intercanthal distance (ICD), shortest distance between the anterior corner of the eyes; 9) Interorbital distance (IOD), distance across top of head between medial margins of orbits at their closest points; 10) Upper eyelid width (UEW), distance from the base of the upper eyelid to the tip of eyelid; 11) Eye diameter (ED), distance between anterior and posterior corner of upper and lower eyelids; 12) Tympanum diameter (TD), horizontal width of tympanum as its widest points; 13) Brachium length (BL), distance from axilla to flexed elbow; 14) Forelimb length (FLL), distance from vent to outer margin of flexed knee; 15) Lower arm length (LAL), distance from the elbow to the tip of the fourth finger; 16) Forearm length (FAL), distance from flexed elbow to base of inner metacarpal tubercle; 17) Hand length (HAL), longest distance from the base of the inner metacarpal to the tip of third finger; 18) Humeral gland (HG), horizontal length of humeral gland; 19) First finger length (1FL); 20) Second finger length (2FL); 21) Third finger length (3FL); 22) Fourth finger length (4FL): distance from proximal margin of the palmar

tubercle to the tip of the finger I, II, III, IV; 23) Hind limb length (HLL), distance from cloacal opening/vent to the tip of toe IV; 24) Femur length (FML), distance from vent to outer margin of flexed knee; 25) Tibia length (TBL), longest distance from outer margin of flexed knee to outer margin of flexed tarsus; 26) Tarsus length (TSL), distance from outer margin of flexed tarsus to base of inner metatarsal tubercle; 27) Foot length (FL), longest distance from the base of the inner metatarsal to the tip of fourth toe; 28) First toe length (1TL), 29) Second toe length (2TL), 30) Third toe length (3TL), 31) Fourth toe length (4TL), and 32) Fifth toe length (5TL): from the inner metatarsal tubercle to the tip of toes I, II, III, IV, and V. Toe-webbing formulae follow Savage & Heyer (1997) with refinements by Guayasamin et al. (2006). Qualitative traits (e.g., head shape, skin texture, coloration were scored with reference to patterns) comparative treatments (Brown & Guttman 2002, Kok & Kalamandeen 2008).

Size correction and statistics. To minimize size effects, all linear variables (except SVL) were converted to relative values (R = character/SVL × 100) for univariate tests and log10-transformed where appropriate. Allometric adjustments followed the "GroupStruct" workflow of Chan & Grismer (2022) to derive size-adjusted residuals for multivariate analyses. Multicollinearity was screened by pairwise correlations; variables with $|r| \ge 0.9$ were examined and, if necessary, reduced to one representative character. Principal-component analysis (PCA) was conducted on centered and scaled variables (correlation matrix) using prcomp in R (R Core Team 2020). We visualized 95% confidence ellipses for species groups and reported loadings for PC1-PC3. For univariate comparisons among species, we used Kruskal-Wallis tests on R-scaled characters followed by Dunn's post-hoc tests with Holm correction ($\alpha =$ 0.05). All analyses were run in R; package versions are provided in the Supplementary Methods. All raw measurements are archived in Supplementary File S5 to ensure reproducibility.

Molecular and phylogenetic analyses. Genomic DNA was extracted from frozen tissues using standard phenol–chloroform procedures (Sambrook et al. 1989) or Serapure (SeraMag beads) methods. We amplified a 444 bp fragment of the mitochondrial 16S rRNA gene using primer pairs H3056/L2606 (Hedges et al. 1993) and 16Sar-L/16Sbr-H (Palumbi et al. 1991); PCR and cycle-sequencing used the same primers.

Chromatograms were edited in Chromas Pro (Technelysium, Sequences Australia). aligned with MAFFT as implemented in UGENE v51.0 (Okonechnikov et al. 2012), with ambiguous positions trimmed to a common length shared by all samples. Model selection for Bayesian Inference (BI), Maximum Likelihood (ML), and Neighbour-Joining (NJ) followed Kakusan3 (Tanabe 2007) under AIC. ML and NJ analyses were performed in MEGA X (Kumar et al. 2018) with 1000 bootstrap replicates and a 50% majority-rule consensus threshold. BI was conducted in MrBayes 3.2.4 (Ronquist et al. 2012) under GTR+ Γ , using two independent runs of four chains each for 10 million generations, sampling every 1000 generations and discarding the first 25% as burn-in. Convergence and mixing were assessed by the average standard deviation of split frequencies (< 0.01) and potential scale-reduction factors (~ 1.0) . Outgroups (Limnonectes sisikdagu and Rhacophorus bengkuluensis) were chosen following Streicher et al. (2014) and Chan et al. for stable rooting of Ranidae (2020b)relationships. Uncorrected p-distances among taxa (Sup. Table 2) were computed in MEGA X with pairwise deletion of gaps.

Mapping and occurrence data. We compiled locality data from our vouchers (MZB and UTA), published records, and GBIF occurrences for named taxa within the *H. signata* complex. Records were harmonized to ASW usage, screened for georeferencing errors duplicates, and mapped in QGIS (Version 3.34) in WGS84. GBIF points were used for visualization only and were not treated as confirmed identifications without voucher or genetic corroboration. GBIF data were cited following official citation guidelines (GBIF.org 2025).

Results

Phylogenetic inference. Analyses of the 444 bp mitochondrial 16S rRNA fragment yielded congruent topologies under Bayesian inference (BI), maximum-likelihood (ML), and neighbourjoining (NJ) methods. The BI tree is presented (Fig. 1) as it represents the consensus topology among all analyses. The Hylarana signata complex formed a monophyletic group relative to the outgroups and split into two principal lineages: a picturata-group (Clade I) and a fantastica-group (Clade II). Within Clade II, the two Sumatran lineages described herein, H. anantambanii sp. nov. and H. hellenae sp. nov.,

each formed well-supported, reciprocally monophyletic clades (BPP 1.00, MLBP 98, NJBP 99), distinct from *H. fantastica*, *H. siberu*, and *H. centropeninsularis*. Within Clade I, *H. sundabarat* was recovered with the picturatasignata assemblage and showed sister-group affinities to *H. picturata* (BPP 0.85, NJBP 100), together forming a larger clade that also included the Philippine taxa *H. grandocula*, *H. similis*, *H. mangyanum*, and *H. moellendorffi*. The resulting topology is consistent with previous multilocus frameworks for *Pulchrana/Hylarana* (Chan *et al.* 2020b).

Genetic distances. Uncorrected p-distances (Sup. Table 2) support the distinctness of the new taxa and clarify relationships within the complex. Divergence between H. anantambanii sp. nov. and H. hellenae sp. nov. is 4.81%. Distances between H. anantambanii sp. nov. and H. fantastica are 9.63-10.55%, and between H. hellenae sp. nov. and H. fantastica are 8.03-9.17%. Within Clade I, H. sundabarat differs from H. picturata by 6.16-9.17% and from H. signata by 6.42-8.49%. These values are consistent with species-level separations commonly reported for ranids based on 16S. Mean within-species divergence across sampled populations was $\leq 1.2\%$, confirming low intraspecific variation.

Morphometrics and ordination. Principalcomponent analysis (PCA) of adult males (Fig. 2) recovered clusters broadly corresponding to nominal taxa. The two new species occupy distinct morphospatial regions within Clade II: H. hellenae sp. nov. tends to plot on the positive side of PC1 and partially overlaps with H. fantastica, whereas H. anantambanii sp. nov. clusters closer to H. picturata, H. siberu, and H. sundabarat. Despite these tendencies, the new species exhibits partial morphometric overlap with congeners, reflecting the subtle external differentiation typical of the group. Post-hoc Dunn tests on size-standardized variables (Sup. significant 3) identified differences for several relative characters (e.g., head width, hand length, upper-eyelid width, finger and toe ratios) in specific comparisons, but no single metric alone diagnoses either new species across all contrasts. Diagnostic separation, therefore, relies on stable combinations of external traits corroborated by mitochondrial differentiation. Eigenvalues for PC1-PC3 explained 74.2% of total variance, with the highest loadings from HL, HW, and UEW.

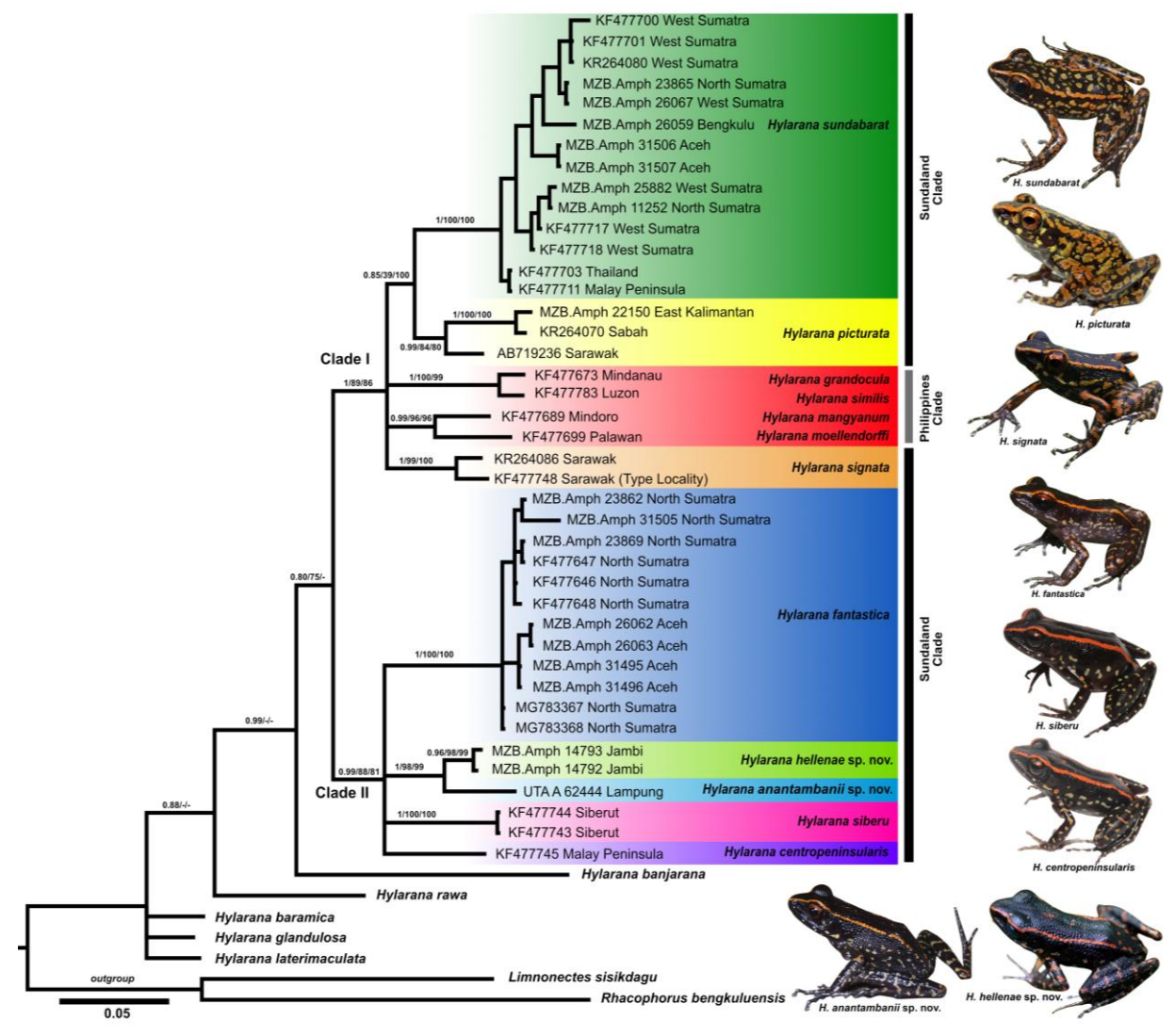


Figure 1. Phylogenetic relationship tree of *Hylarana signata* complex and related species, based on the Bayesian inference tree estimate from 444 bp of 16S rRNA mtDNA gene. Sample numbers and localities are included in Sup. Table 1. Numbers above the branch represent bootstrap supports for Bayesian Posterior Probabilities (BPP) / Maximum Likelihood Bootstrap Proportion (MLBP) / Neighbour Joining Bootstrap Proportion (NJBP). Photo credits: Misbahul Munir (*H. sundabarat, H. picturata, H. fantastica, H. siberu, H. centropeninsularis*), Eric N Smith (*H. anantambanii* sp. nov.), Amat Ribut (*H. signata*)

Distributional evidence. Mapped occurrences (Fig. 3) and examined vouchers indicate that *H. anantambanii* sp. nov. is restricted to southern Sumatra, with confirmed material from Kubu Perahu, West Lampung (Lampung Province), and additional records from South Bengkulu (Bengkulu Province). The species occurs in geographic proximity to *H. sundabarat*, and local sympatry or near-sympatry is plausible based on mapping. *Hylarana hellenae* sp. nov. is currently known from central-western Sumatra (Kerinci Seblat National Park, Jambi Province) and based on available material, does not co-occur with other members of the complex at that site. Newly generated genetic vouchers attributable to *H.*

sundabarat confirm its presence on Sumatra and, together with museum records summarized in Sup. Table 1, indicate a distribution spanning at least Aceh, North Sumatra, West Sumatra, and Bengkulu. All distribution points georeferenced in WGS84 and cross-checked against GBIF occurrence records cited following GBIF.org (2025). GBIF-only points were used for visualization and require voucher or genetic corroboration before inclusion in formal range statements. Both new species were recorded within protected forest areas—Bukit Barisan Selatan National Park and Kerinci Seblat National Park—suggesting persistence relatively undisturbed habitats.

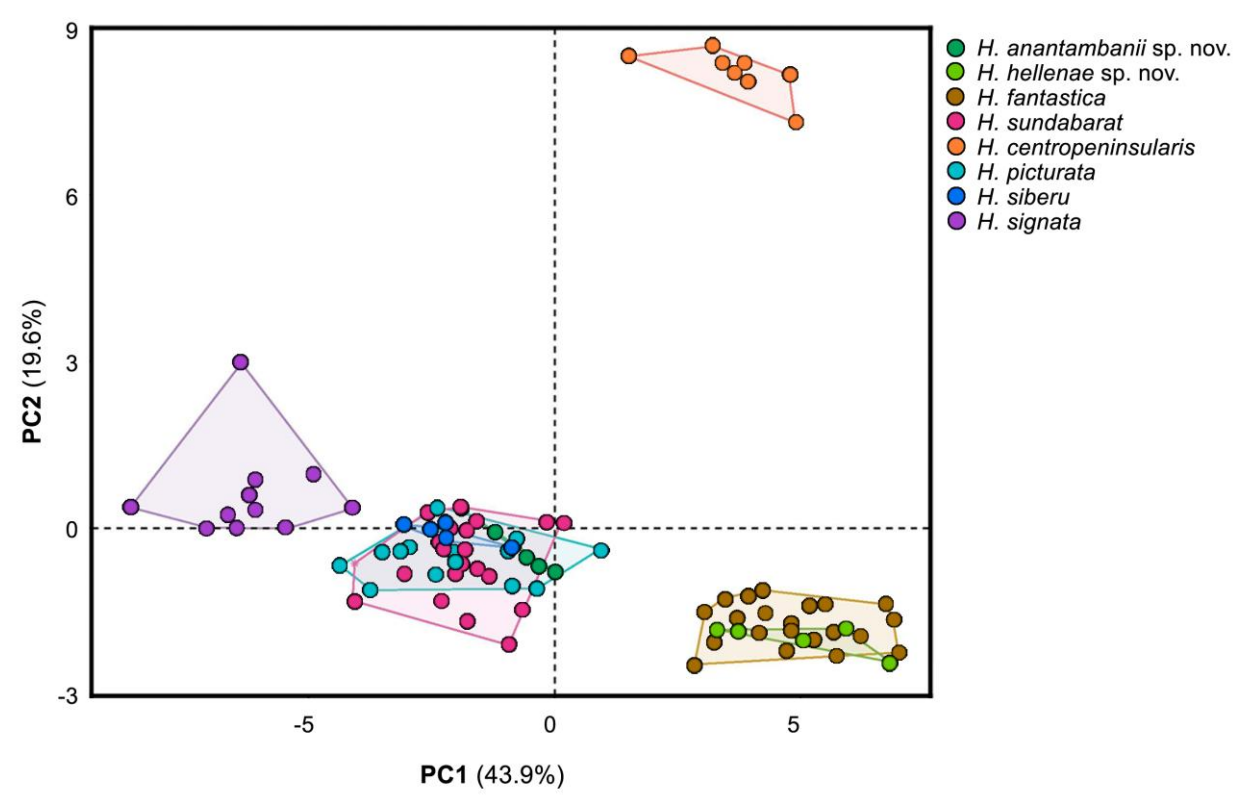


Figure 2. Visualization of Principal Component Analysis (PCA) based on morphometric data of several *Hylarana signata* complex specimens with a 95% confidence level.

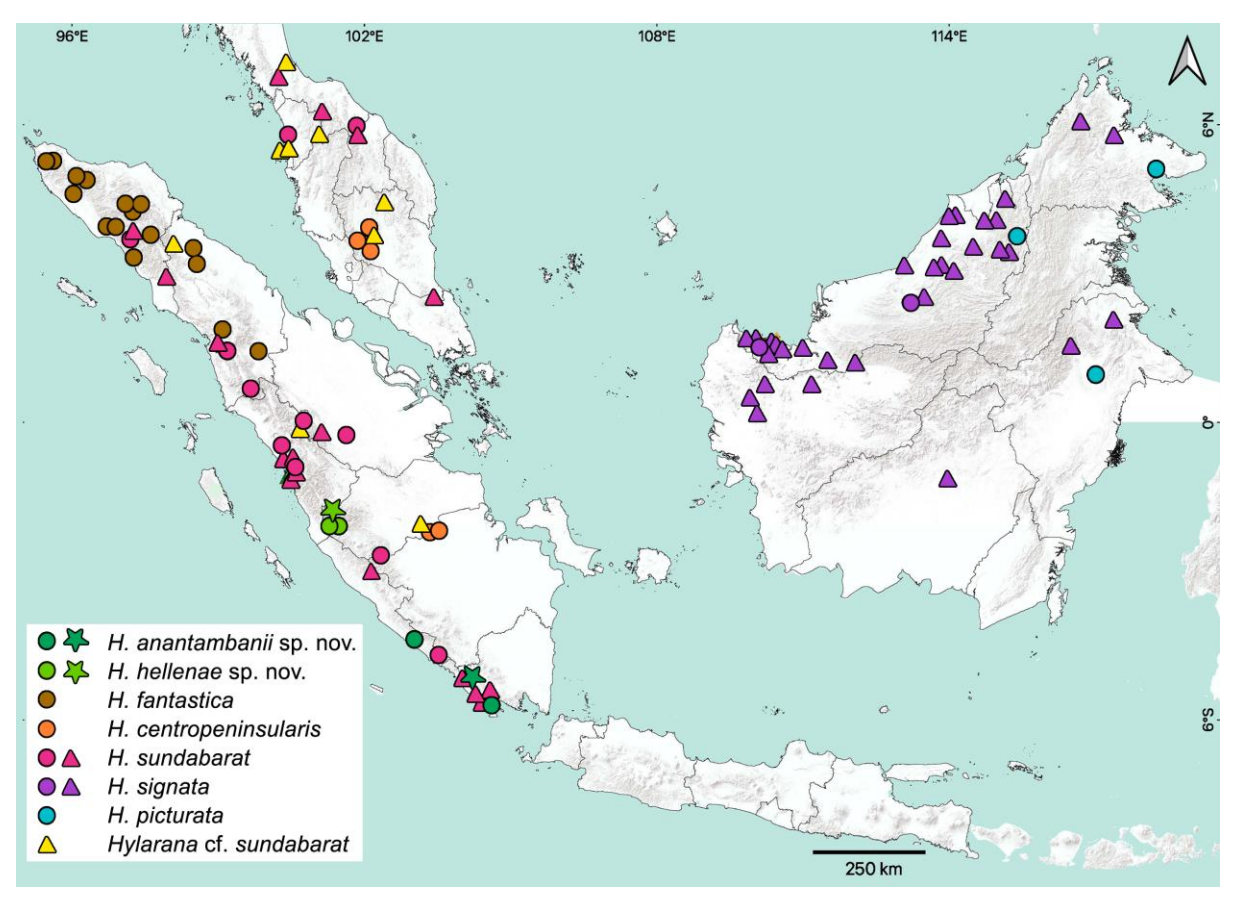


Figure 3. Distribution of the *Hylarana signata* complex in Sundaland. Each dot indicates records of museum/literature; stars mark the holotype localities; triangles indicate GBIF occurrences. Coordinates referenced to WGS84. GBIF points are for visual context only and were not treated as confirmed identifications without voucher or genetic support.

Taxonomy

Hylarana anantambanii sp. nov. (Figs. 1–3, 4A, 5-I, 6-I; Sup. Table 4) [urn:lsid:zoobank.org:act:6DBA8723-9960-4274-ABC8-CB66DDF7A773]

Rana signata — Mistar 2003: 61, Fig. 44

Holotype. MZB.Amph 3481 (Fig. 5-I), an adult male collected from Kubu Perahu, Bukit Barisan Selatan National Park, Lampung, Indonesia by Andiek Fajar on 17 February 1998.

Paratype (n=3). MZB.Amph 4065–4066, an adult male collected from Air Sumur Melintang, Pino Raya, Bengkulu Selatan, Bengkulu, Indonesia by Alfad Y. on 14 September 1999, and UTA A 62444, an adult male collected from Kubu Perahu (5.06011°S, 104.03222°E; alt. 880 m a.s.l.), Lampung Barat, Lampung, Sumatra, Indonesia by A. Hamidy and Eric N. Smith on 14 January 2014.

Diagnosis. The following unique combinations of characters distinguish Hylarana anantambanii sp. nov., from its congeners: (1) a medium sized frog, SVL adult males (n = 5)34.87–41.67 mm; (2) males with medium humeral glands (2.78-3.85 mm), oval, center (Fig. 6-I C); (3) nuptial pads absent; (4) dorsal skin finely granular to granulated, with keratinised white asperities at tip of each granule; (5) webbing formula: I $2-2\frac{1}{2}$ II 2-3 III $2\frac{1}{3}$ $3 \frac{1}{2}$ IV $3 \frac{2}{3} - 2 \frac{1}{3}$ V (Fig 3. IC); (6) dorsolateral stripe, thin (0.48–0.59 mm), orange, continuous; (7) middorsum black with a combination of spot that form a dotted line in the center; (8) bars on flanks and dorsal surface limbs, cream to faded orange compared to dorsolateral; (9) femoral gland, small, less developed (Fig. 6-I A); (10) skin of venter smooth, dark brown with small light dots, (11) iris background black, with orange-golden line encircling pupil; (12) upper and lower lip with cream to yellow spots (upper lip: 3–4; lower lip: 3).

Description of holotype. An adult male, SVL 34.87 mm; large humeral gland (HG/BL = 37.72%); nuptial pad absent; body slender; head longer than wide (HL/HW = 118.58%); snout obtusely pointed in dorsal view, slightly protruding in lateral view; canthus rostralis sharp, constricted behind nares; loreal region sloping, deeply concave; vomerine teeth distinct; eye diameter > interorbital distance (ED/ IOD = 141.01%); internarial distance < interorbital distance (IND/IOD = 77.47%); tympanum

diameter < eye diameter (TD/ED=59.78%); supratympanic fold conspicuous.

Dorsum granulated with white tipped keratinized asperities: flanks granular with white tipped keratinized asperities; venter smooth; forelimb relatively slender. Brachial length less than forearm length (BL/FAL = 82.93%); fingers long and slender, without webbing; finger length II<IV<I<III, 1FL/2FL = 127.32%, 1FL/4FL = 103.25%, Finger III longest; fingertips slightly expanded into rounded disc, circummarginal groove present; subarticular tubercles present, round, prominently; raised number subarticular tubercle for each finger: I(1), II(1), III(2), IV(2); supernumerary tubercles between the base of each finger, smaller and less prominent subarticular tubercles, than translucent; outer palmar tubercle elongate, inner metacarpal tubercle oval or rounded, inner palmar tubercle longer than outer palmar tubercle (IPTL/OPTL=163.06%).

Hindlimbs long, tibia shorter than femur (TBL/FML = 106.73%); relative length of femur, tibia, and tarsus, to SVL is 52.82%, 56.38%, and 27.16%, respectively; skin texture of dorsal side of anterior thigh to posterior tarsal finely granulated; tip of toes expanded, circummarginal groove present; subarticular tubercles distinct, round, highly elevated, translucent; number of subarticular tubercle for each toe: I(1), II(1), III(2), IV(3), V(2); toe length: I<II<V<III<IV, 1TL/2TL=85.53%, 1TL/4TL=29.36%, 3TL/5TL = 101.16%; outer metatarsal tubercle raised, oval, translucent; inner metatarsal tubercle distinct and long, elevated, translucent, larger than outer metatarsal tubercles (IMTL/ OMTL = 178.26%); webbing formula: (4) webbing formula: I 2 $- 2 \frac{1}{2}$ II 2 - 3 III 2 $\frac{1}{2} - 3$ 2/3 IV 3 $2/3 - 2 \frac{1}{3} V$.

Coloration. In life (Fig. 4A), dorsum black with few markings; dorsolateral line thin, 100% straight; middorsal coloration with 66.7% dark brown unmarked, 33.3% dark brown with yellow to orange spot on the vertebrae; flanks and dorsal side of limbs with thin to medium bar pale cream to pale orange; ventral and throat coloration with 44.4% pale brown with white spot, 65.5% dark brown with white spot.

In preservative (Fig. 5-I), dorsum uniformly dark brown to blackish; continuous dorsolateral stripes cream lines extending from the posterior edge of the upper eyelids to the posterior of shank; a cream thin and often fragmented middorsal stripe on vertebrae; forelimbs with pale cream blotches until digits; hind limbs with

well-defined pale 8-11 transverse bands across the thigh, shanks, and foot. Ventrum with medium to dark brown, with numerous, irregularly scattered pale cream blotches of varying sizes extending across the chin, abdomen, anteroventral thigh to foot.

Variation. We observed variation among five adult male specimens of *Hylarana anantambanii* sp. nov. The dorsal texture in adults has tipped keratinised asperities. Dorsolateral width 0.48–0.59 mm. The webbing formula is I $2 - 2 \frac{1}{2}$ II 1 $\frac{1}{3} - 2^{2} - 3$ III $2 \frac{1}{2} - 2 \frac{1}{3} - 3 \frac{1}{2}$ IV $3 \frac{1}{2} - 3 \frac{2}{3} - 2 - 2 \frac{1}{3}$ V.

Etymology. The specific epithet anantambanii is a noun in the genitive singular, honouring Anant Ambani, an Indian businessman and animal-welfare advocate, in recognition of his unwavering passion and extraordinary dedication to the care, rescue, and rehabilitation of wildlife across the globe. Through the visionary initiative Vantara, he has created a sanctuary of hope and healing—a place where injured, abandoned, and endangered animals find refuge and a renewed chance at life. The name is formed from the combined name "Anant Ambani", adding the masculine genitive suffix -i (ICZN Art. 31.1.2).

Comparison. Based on our phylogenetic tree and the distribution of the Hylarana signata complex on Sumatra Island, we compared H. anantambanii sp. nov., H. fantastica, H. siberu, H. centropeninsularis, and the sympatric species H. sundabarat (see Fig. 1 & 3; Sup. Table 4). Hylarana anantambanii sp. nov. and H. fantastica can be distinguished from Н. centropeninsularis and H. siberu by the following qualitative characters (Fig. 4): a narrow dorsolateral stripe (vs broad), pale orange to cream in colour (vs bright orange to reddish); the middorsal region contains faint lines or small blotches (vs unmarked); the lateral body surface bears small, pale yellow blotches (vs larger vellow to light vellow blotches); the thigh to shank region displays faint bars in cream to pale orange (vs without or less developed bars, medium to large blotches in yellow or bright orange). Furthermore, *H. anantambanii* sp. nov. and *H. fantastica* can be distinguished from *H*. picturata, H. signata, and H. sundabarat by the middorsal pattern, which is faint or limited (vs numerous bright spots), and by a narrow, dorsolateral stripe (vs broad, continuous continuous, nearly continuous, or absent stripe).

Morphometrically in males, H. anantambanii sp. nov. differs from H. fantastica by shorter snout length, SL 5.09–5.54, mean 5.31 \pm 0.20

mm (vs slightly longer until very long, 5.28–6.91 mm, mean 5.96 ± 0.45 mm: Arifin et al. (2018) 6.5-7.00 mm, mean 6.79 ± 0.16 mm); shorter distance snout to nostril SNL 1.38-1.81 mm, mean 1.49 ± 0.25 mm (vs slighty longer, 1.62– 2.18 mm, mean 1.87 ± 0.20 mm: Arifin et al (2018) 2.2-2.70 mm, mean $2.51 \pm 0.16 \text{ mm}$) with RSNL 2.76–4.34 %, mean 3.78 ± 0.04 % (vs medium to longer, 3.55-5.08 %, mean $4.34 \pm$ 0.43); narrow inter canthal distance, ICD 5.53-6.16 mm, mean $5.75 \pm 0.24 \text{ mm}$ (vs wider, 5.80– 7.69 mm, mean 6.73 ± 0.59 mm); narrower upper eyelid width, RUEW 7.46–9.09 %, mean 8.43 \pm 0.27 % (vs slightly wider, 8.37–10.77 %, mean 9.37 ± 0.68 %); colouring ventrum with dark brown, white spots (vs white to cream, with white spots); dorsum of thigh-shank to the posterior tarsus with clearly white bars (vs bars unclear and small blotches in middle shanks to the posterior tarsus); humeral gland oval, concentrated in the centre of the upper arm (vs triangle view from above, enlarged and concentrated distally or towards the elbow) (Fig. 6); foot with shorter tarsal length, TSL 9.47-11.12 mm, mean 10.40 ± 0.80 mm (vs slightly longer, 10.80-13.30 mm, mean 12.25 ± 0.79 mm: Arifin et al (2018) 11.2–13.9 mm, 12.3 \pm 0.8 mm) with RTSL 25.07-27.16 %, mean 26.30 \pm 1.48 % (vs longer, 26.59–30.70 %, mean 28.44 \pm 1.20 %); smaller to medium outer palmar tubercle, ROPTL 2.70–4.35 %, mean 3.47 ± 0.83 (vs medium to larger, 3.66–5.20 %, mean 4.19 \pm 0.44 %).

Hylarana anantambanii sp. nov. differs from H. siberu by shorter snout length, RSL 12.41-15.06%, mean $13.47 \pm 1.27\%$ (vs slightly longer, 14.77-16.59%, mean 15.96 ± 0.72); shorter snout to narial length, RSNL 2.76-4.34%, mean 3.78 \pm 0.04% (vs longer, 4.27–5.44%, mean 4.91 \pm 0.44%); narrow intercanthal distance, RICD 13.70-16.20%, mean $14.60 \pm 1.27\%$ (vs wider, 16.82-18.02%, mean $17.26 \pm 0.48\%$); body on the dorsum surface slightly rough, with small tubercle with asperities (vs smooth, slightly larger without asperities); colouring ventrum with dark brown, white spots (vs light brown, without light spots); thin dorsolateral stripe, slightly not continued (vs larger dorsolateral, full continued); thigh to the shank with small tubercle with asperities, white stripes (vs very smooth, white spots); hand with small oval humeral gland (vs longer); shorter tarsal length, RTSL 25.07– 27.16%, mean $26.3 \pm 1.48\%$ (vs longer, 28.50– 32.91%, mean $30.59 \pm 1.72\%$); webbing on third to fifth toe [3 III 2 $\frac{1}{2}$ - 2 $\frac{1}{3}$ - 3 $\frac{1}{2}$ IV 3 $\frac{1}{2}$ - 3 $\frac{2}{3}$ -

2 - 2 $\frac{1}{3}$ V (vs 3 III 2 - 3 $\frac{1}{2}$ IV 3 - 2 V)] (Fig. 5-I vs 5-IV).

Hylarana anantambanii sp. nov. differs from H. centropeninsularis by shorter snout length, RSL 12.41–15.06%, mean $13.47 \pm 1.27\%$ (vs longer, 14.43–16.23%, mean 15.41–0.58%); narrow intel canthal distance, RICD 13.70-16.20%, mean $14.60 \pm 1.27\%$ (vs broad, 19.94– 18.70%, mean $16.91 \pm 1.15\%$); shorter head length compare to head width, HL/HW 109.20-118.58%, mean 114.60 \pm 3.49% (vs longer, 119.30–132.54%, mean 128.95 \pm 5.34%); shorter toe length (vs longer): R1TL 8.02–10.23%, mean 8.82 ± 0.14 (vs 14.98–17.56%, mean 16.21 \pm 0.76%); R2TL 10.27-11.93%, mean $11.00 \pm$ 1.18% (vs 21.41-24.75%, mean $23.16 \pm 1.27\%$); R3TL 16.15–20.02%, mean $17.65 \pm 1.24\%$ (vs 32.27-35.88%, mean $33.55 \pm 1.30\%$); R5TL 17.46-19.79%, mean $18.23 \pm 1.65\%$ (vs 33.02-35.94%, mean $34.19 \pm 1.04\%$) (Fig. 5-I vs 5V).

Hylarana anantambanii sp. nov. morphology differs from H. sundabarat by body on dorsum with small tubercle with asperities, without blotches or spots, only slightly on middorsal (vs smooth, with large white blotches or spots); thin dorsolateral stripe (vs slightly thick); hand with little white blotches (vs much, larger white blotches); dorsum hindlimb with white small bars (vs white large blotches); small and oval humeral gland, center from upper arm (vs very small, slightly not distinct, concentrated distally from the upper arm); toes half webbed: I 2 - 2 ½ II 1 ½ - 2 - 3 III 2 ½ - 2 ½ - 3 ½ IV 3 ½ - 3 2/3 - 2 - 2 ½ V (vs almost full: I 1 ½ - 2 II 1 ⅓ - 2 ½ III 1 ½ - 2 IV 2 2/3 -1 V) (Fig. 5-I vs 5VI).

Tadpoles and acoustics. Unknown

Distribution and natural history. Hylarana anantambanii sp. nov. is currently known from two locations, in South East Sumatra, Lampung Province (Bukit Barisan Selatan National Park, Kubu Perahu, West Lampung) (Fig. 3), and Bengkulu Province (Air Sumur Melintang, Pino Raya, South Bengkulu). The holotype was found at high elevation (880 m asl). Paratype from Pino Raya was collected from a lower elevation near the community village.

Hylarana hellenae sp. nov.

(Figs. 1–3, 4B, 5-II, 6-II; Sup. Table 4) [urn:lsid:zoobank.org:act:2A3E22B9-521A-4D55-9028-190412CAD017]

Rana siberu — Kurniati 2008: 65, Fig. 75

Holotype. MZB.Amph 14792 (field number HK 1031, Fig. 5-II), an adult male collected from

Kerinci Seblat National Park (-2.097778, 101.249361; alt. 500 m a.s.l.), Tapan, Jambi, Sumatra, Indonesia by Hellen Kurniati on 23 February 2005.

Paratype (n=3). MZB.Amph 14791 (HK 1020), MZB.Amph 14793 (HK 1025), and MZB.Amph 14794 (HK1026) adult males collected from the same locality as the holotype, by Hellen Kurniati on 23 and 24 February 2005.

Diagnosis. The following combinations of characters distinguish Hylarana hellenae sp. nov., from its congeners: (1) a medium sized frog; SVL adult males (n = 7)41.16-43.23 mm; (2) males with medium humeral glands (3.16–4.21 mm), oval or triangle, concentrated proximally; (3) nuptial pads absent; (4) dorsal clearly granulated, with keratinised white asperities at tip of each granule (Fig 3. IIA); (5) webbing formula: I $2-2^{1/2}$ II 1 $2/3 - 2^{-}$ 3 III 2 - $2^{1/3}$ - $3^{1/2}$ IV $3^{1/2}$ - 2 - 2 ½ V; (6) dorsolateral stripe, thin (0.58–0.86 mm), orange, continuous, anteriorly confluent and posteriorly interconnected by spots; (7) middorsum black with a combination of spots that form a dotted line in the centre; (8) bars on shank and dorsal surface thigh, cream to pale orange compared to dorsolateral; (9) femoral gland, medium (Fig. 6-III A); (10) skin of venter smooth, lightly brown without spots.

Description of Holotype. An adult male, SVL 42.29 mm; large humeral gland (HG/BL = 49.01%) on anteroventral surface of brachium, paired internal subgular vocal sacs, nuptial pad absent; body slender; head longer than wide (HL/HW = 112.82%); snout obtusely pointed in dorsal view, slightly protruding in lateral view; canthus rostralis sharp, constricted behind nares; loreal region sloping, deeply concave; vomerine teeth distinct, tongue lanceolate; eye diameter > interorbital distance (ED/ IOD = 152.08%); internarial distance < interorbital distance (IND/IOD = 80.56%); tympanum diameter < eye diameter (TD/ED=58.30%); supratympanic fold conspicuous.

Dorsum is granular with white-tipped keratinized asperities; flanks are granular with white-tipped keratinized asperities; the venter is smooth; the forelimb is relatively slender. Brachial length less than forearm length (BL/FAL = 82.93%); fingers long and slender, without webbing; finger length: II < I < IV < III, 1FL/2FL = 109.4%, 1FL/4FL = 74.41%, Finger III longest; fingertips slightly expanded into rounded disc, circummarginal groove present; subarticular tubercles present, round, raised

prominently; number of subaticular tubercle for each finger: I(1), II(1), III(2), IV(2); one supernumerary tubercles between the base of each finger, distinct but smaller and less prominent than subarticular tubercles, translucent; outer palmar tubercle elongate, inner palmar tubercle oval, inner palmar tubercle slightly shorter than outer palmar tubercle IPTL/OPTL= 95.41%.

Hindlimbs long, tibia shorter than femur (TBL/FL = 105.49%); relative length of femur, tibia, and tarsus, to SVL is 50.74%, 55.9%, and 28.45%, respectively; skin texture of dorsal side of anterior thigh to posterior tarsal is rough and clearly granulated; tip of toes expanded, circummarginal groove present; subarticular tubercles distinct, round, highly elevated. translucent; number of subarticular tubercle for each toe: I(1), II(1), III(2), IV(3), V(2), toe length: I<II<V<III<IV, 1TL/2TL =91.93%, 1TL/4TL = 35.26%, 3TL/5TL = 96.48%; outer metatarsal tubercle raised, oval, translucent; inner metatarsal tubercle distinct and long. elevated, translucent, larger than outer metatarsal tubercles (IMTL/ OMTL = 191.01%); webbing formula: I $2 - 2\frac{1}{2}$ II $2^{-} - 3$ III $2\frac{1}{3} - 3\frac{1}{2}$ IV $3\frac{1}{2} - \frac{1}{2}$ 2 V.

Coloration. In life (Fig. 4B, not collected), dorsum black with few markings; dorsolateral line thin, pale orange, 100% straight; middorsal coloration dark black and unmarked, with reddish orange spot on the vertebrae; lateral body less marked with small blotches, colouring like dorsolateral stripes; thigh and dorsal side of shank with thin to medium bar reddish orange.

In preservative (Fig. 5-II), dorsum brown to dark brown with contrasting pale markings, including a distinct dorsolateral cream stripe extending from the eyelids to the groin, and a narrow cream middorsal stripe. Forelimbs with cream 8-9 transverse bands, clearly visible along the arm and extending to the digits. Hind limbs with broader pale bands on the thigh, shank, and foot. Ventrum shows uniform light beige to pale brown coloration with minimal dark pigmentation; chin, abdomen, and antero-ventral thigh unmarked, smooth, and pale; shank to foot pale brown with less light scattered.

Variation. We observed variation in four specimens of *Hylarana hellenae* sp. nov. only in adult males. The dorsal texture in adults has tipped keratinised asperities. Dorsolateral width 0.58-0.86 mm. The webbing formula is: I 2 - 2 $\frac{1}{2}$ II 1 $\frac{2}{3}$ - $\frac{2}{3}$ - 3 III 2 - 2 $\frac{1}{3}$ - 3 $\frac{1}{2}$ IV 3 $\frac{1}{2}$ - 2 V.

Etymology. The specific epithet hellenae is a noun in the genitive singular, honouring Hellen Kurniati, an Indonesian herpetologist, at the Museum Zoologicum Bogoriense (LIPI/BRIN), for her dedication over more than 36 years and her long-term field surveys and foundational documentation of Sumatra's herpetofauna, as her stewardship of national well as herpetological collections; she collected the holotype and associated series of this species at Tapan, Jambi. We explicitly treat "Hellen" as a modern personal name (not as the classical Latin Helen), adding the feminine genitive suffix -ae (ICZN Art. 31.1.2).

Comparisons. Hylarana hellenae sp. nov. H. anantambanii sp. nov. H. fantastica differs from H. siberu and H. centropeninsularis by body on dorsum with small blotches or spots and with middorsal stripes performed from spots, from near cloaca to posterior inter orbital, thin dorsolateral stripes; smaller humeral gland, oval or triangle, doesn't fulfil the humeral (vs without blotches and middorsal stripes, thick dorsolateral stripes; larger or long humeral gland, elongated, fulfil the humeral) and H. sundabarat has many blotches but without performed middorsal stripe, thick dorsolateral stripes and humeral gland not developed (see Fig. 4 & 5; Sup. Table 4).

Hylarana hellenae sp. nov. differs from H. anantambanii sp. nov. in life, with a dark black body (vs slightly pale black); reddish orange dorsolateral stripe (vs yellow to pale orange); blotches in lateral body, on upper to lower arm, and a bar on thigh to shank colouring the same as dorsolateral stripe (vs different colour, pale) (Fig. 4B vs 4A). In preservative by dorsum body has rough tubercle with asperities (vs smooth tubercle with asperities) (Fig. 6-II B vs 6-I B); throat with colouring light brown, spotless on the ventrum part (vs dark brown, white spots); dorsum of thigh to the shanks with rough tubercle with asperities (vs smooth tubercle with asperities); wider head width, RHW 33.03-35.97%, mean $34.82 \pm 1.32\%$ (vs narrower, 31.58-33.95%, mean $32.55 \pm 1.61\%$); wider intercanthal distance, RICD 15.89–17.45%, mean $16.56 \pm 0.75\%$ (vs 13.70-16.20%, mean $14.60 \pm 1.27\%$); humeral gland oval or triangle, concentrated proximally or toward the angle of the upper arm (vs oval, concentrated in the middle part of the upper arm) (Fig. 6-II C vs 6-I C); small outer palmar tubercle, ROPTL 2.70-4.35 mm, $3.47 \pm 0.83 \text{ mm}$ (vs larger, 4.30-5.15mm, 4.62 ± 0.37 mm); toe webbing: II 1 $2/3 - 2^{-}$

Plate 25



Figure 4. Adult males of selected species of *Hylarana signata* complex in life from Sumatra: **(A)** *H. anantambanii* sp. nov. (holotype, field no. ENS 14833), **(B)** *H. hellenae* sp. nov. (Tapan, not collected), **(C)** *H. fantastica* (field no. ENS 16534), **(D)** *H. centropeninsularis* (field no. MUN 01074), **(E)** *H. siberu* (field no. MUN 01417), and **(F)** *H. sundabarat* (MZB.Amph 20945); © Photo: E.N. Smith (A), H. Kurniati (B), M. Munir (C–F).

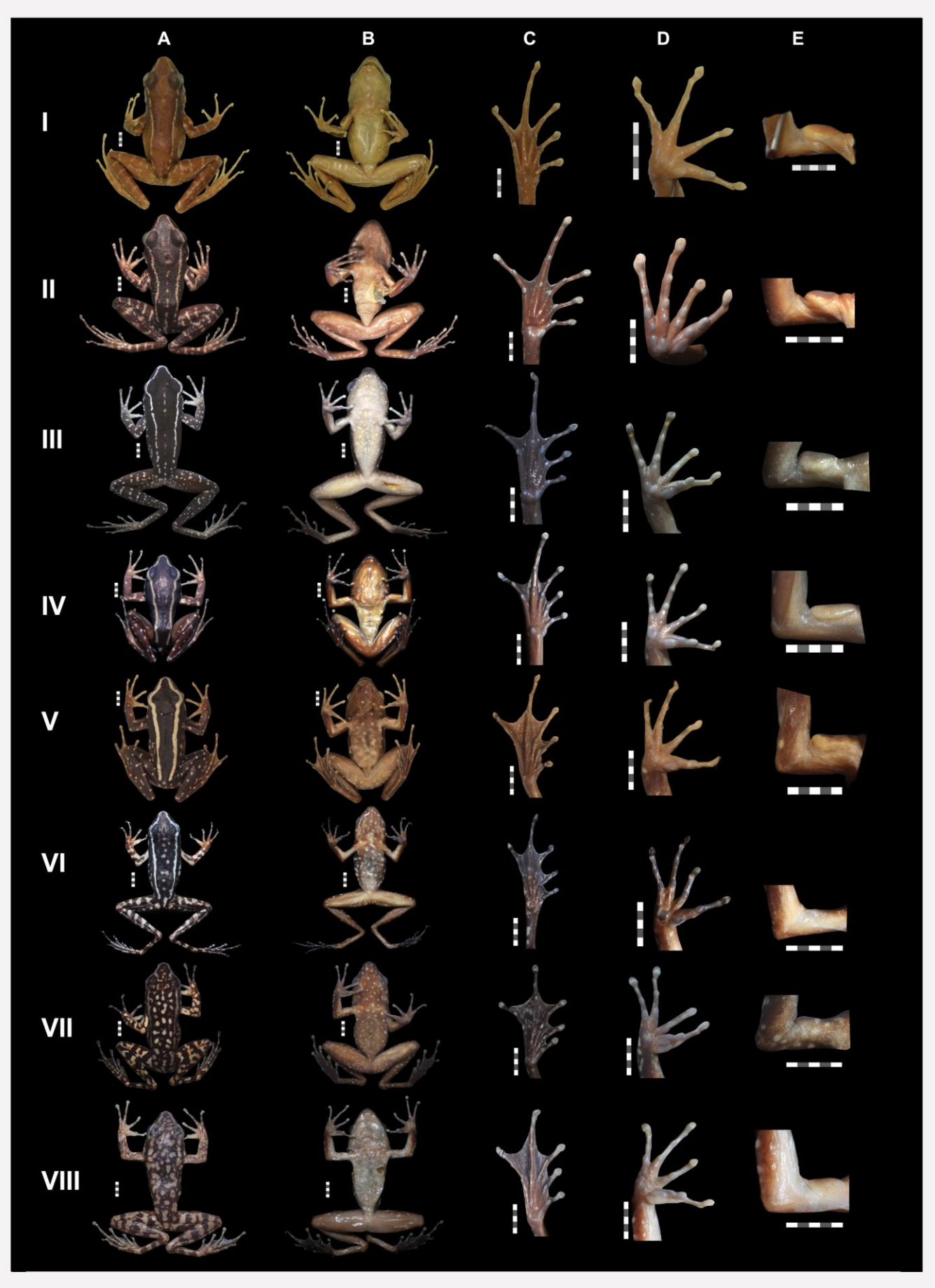


Figure 5. Comparative morphology of adult males in the *Hylarana signata* complex: (A) dorsal and (B) ventral body, (C) ventral foot (right), (D) ventral hand (right), (E) humeral gland of (I) *H. anantambanii* sp. nov. (UTA A62444), (II) *H. hellenae* sp. nov. (MZB.Amph 14792), (III) *H. fantastica* (MZB.Amph 31505), (IV) *H. siberu* (MZB.Amph 10676), (V) *H. centropeninsularis* (MZB.Amph 28764), (VI) *H. signata* (MZB.Amph 6267), (VII) *H. sundabarat* (MZB.Amph 20945), (VIII) *H. picturata* (MZB.Amph 15258); scale: 5 mm.

Plate 27

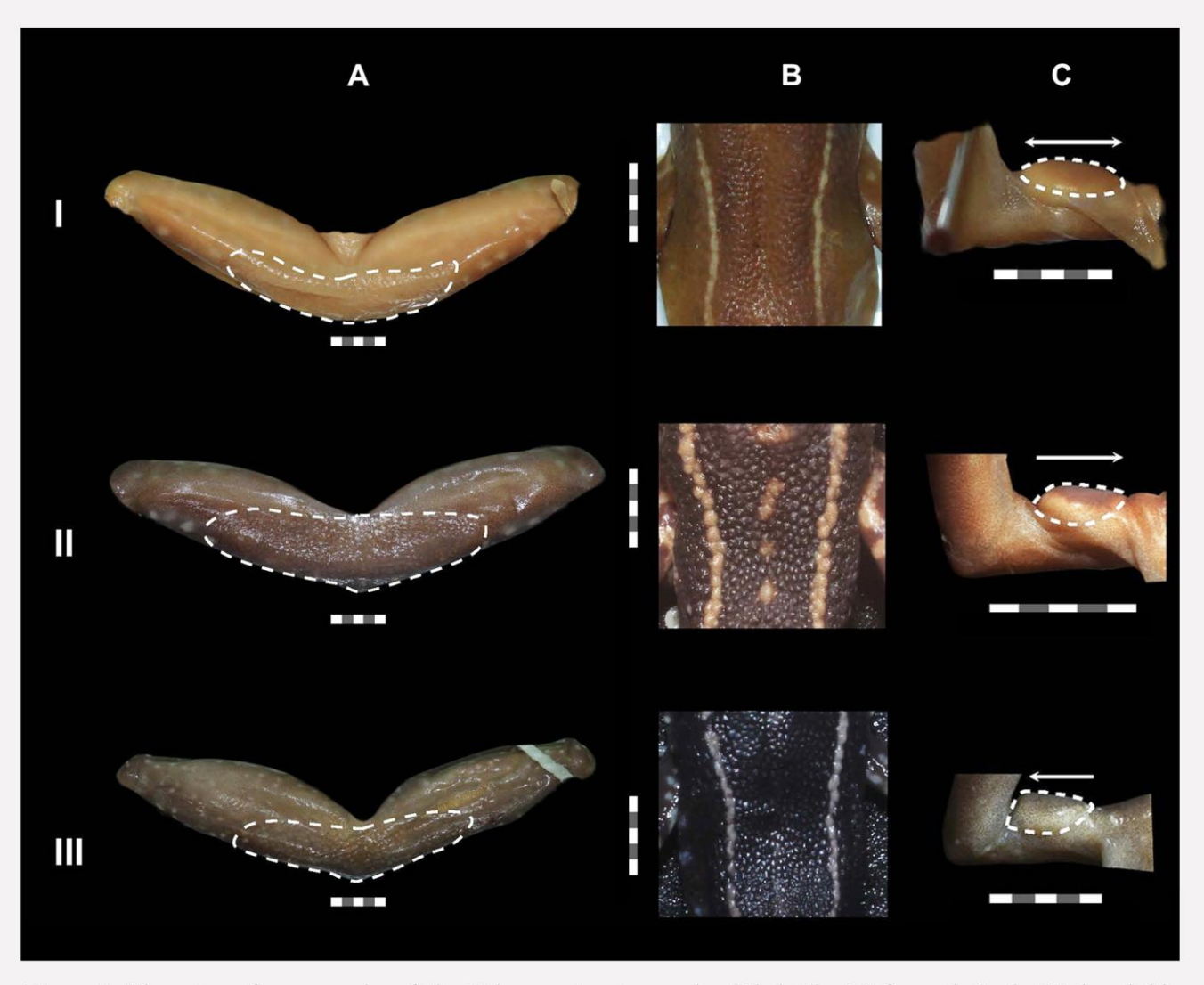


Figure 6. Characters of some species of the *Hylarana signata* complex (Clade II): **(A)** femoral gland, **(B)** dorsal skin textures, **(C)** humeral gland of **(I)** *H. anantambanii* sp. nov. (MZB.Amph 3481), **(II)** *H. hellenea* sp. nov. (MZB.Amph 1492, **(III)** *H. fantastica* (MZB.Amph 31505): scale: 5 mm

3 III 2 - 2 $\frac{1}{3}$ - 2 V (vs II 1 $\frac{1}{3}$ - 2 - 3 III 2 $\frac{1}{2}$ - 2 $\frac{1}{3}$ - 2 - 2 $\frac{1}{3}$ V) (Fig. 5-II vs 5-I, Sup. Table 4).

Hylarana hellenae sp. nov. differs from H. fantastica in preservative by dorsum having rough tubercle with asperities, completely (vs smooth tubercle with asperities, concentrated in the middorsal to near the cloacal opening); throat with light brown colouring, spotless on the ventrum part (vs white creamy, with white little spots) dorsum of thigh to the shanks with rough tubercles with asperities, clearly white to pale orange bar (vs smooth tubercle with asperities, small white blotches or sometimes forming orange bar which is similar colouring to the dorsolateral stripes); larger humeral gland, concentrated on proximal part of upper arm (vs small, concentrated on distal part of upper arm) (Fig. 6-II C vs 6-III C); larger outer palmar tubercle, elongated (vs small, oval) (Fig. 5-II vs 5-III).

Hylarana hellenae sp. nov. differs from H. siberu by larger body size, SVL 41.68-43.23 mm, mean 42.40 ± 0.64 mm (vs smaller, 35.08– 37.26 mm, mean $36.42 \pm 0.93 \text{ mm}$); larger eye diameter, RED 15.02 ± 1.11% Leong & Lim (2004) RED 14%); body on the dorsum surface rough, with larger tubercle with asperities (vs smooth, tubercle without asperities), with middorsal spot performed stripe (vs without middorsal stripe); medium dorsolateral stripes (vs larger dorsolateral stripes); thigh to the shank with larger tubercle with asperities, white small bars (vs very smooth, small white blotches); larger oval humeral gland, concentrated on proximal part of upper arm (vs longer, almost filling the upper arm) (Fig. 5 II vs IV); different webbing formula on third to fourth finger: III 2 $\frac{1}{3} - \frac{3}{2} \text{ IV } \frac{3}{2} \text{ (vs III } 2 - \frac{3}{3} \text{ IV } \frac{3}{3} \text{), corner of }$ webbing between fourth to fifth toes, more inward (vs outward) (Fig. 5-II vs 5-IV).

Hylarana hellenae sp. nov. differs from H. centropeninsularis by wider head width, RHW 31.58-35.97%, mean $33.77 \pm 1.66\%$ (vs narrower, 27.79-32.48%, mean $29.58 \pm 1.73\%$); smaller head length compared to head width HL/HW 109.22-118.54%, mean $112.40 \pm 3.26\%$ (vs larger, 119.26-132.54%, mean $128.95 \pm 5.34\%$); longer hand length, RHAL 29.01-32.68%, mean 30.58 ± 1.31 (vs very shorter, 26.07-27.96%, mean $27.10 \pm 0.61\%$); longer foot length, FL 20.48-22.98 mm, mean 22.16 ± 1.14 mm (vs shorter, 17.40-19.49 mm, mean 18.45 ± 0.96 mm: Chan et al. (2014) and Arifin et al. (2018) 17.5-19.9 mm, mean 18.12 ± 1.01) (Fig. 5-II vs 5-V).

Hylarana hellenae sp. nov. differs from H. sundabarat by larger head width, RHW 31.58-35.97%, mean 33.77 \pm 1.66% (vs slightly smaller, 29.25-32.67%, mean $31.16 \pm 1.07\%$); shorter head length compared to head width, HL/HW 109.22–118.54%, mean $112.40 \pm 3.26\%$ (vs longer, 114.23-132.96%, mean $123.80 \pm$ 5.43); dorsum with larger tubercle with asperities, without blotches or spots, only slightly on middorsal (vs smooth, with large white blotches or spots); clear dorsolateral stripe (vs camouflaged by blotches); overall ventrum including hand and hindlimb with light brown colouring, without little spots (vs slightly dark brown, with little spots); longer brachial length, BL 8.59-10.18 mm, mean 9.07 ± 0.74 mm (vs shorter, 6.87-8.71 mm, mean 7.59 ± 0.50 mm) with larger, concentrated proximally from the upper arm (vs very small, slightly not distinct, concentrated distally from the upper arm); longer forearm length, FAL 9.76-10.58 mm, mean 10.21 ± 0.44 mm (vs shorter, 7.71–9.84 mm, mean 8.69 ± 0.54 mm); toes half webbed: I 2-2 $\frac{1}{2}$ II 1 2/3 - 2⁻ -3 III 2 - 2 2/3 -3 $\frac{1}{2}$ IV 3 $\frac{1}{2}$ - 2 V (vs almost full: I 1 $\frac{1}{2}$ – 2 II 1 $\frac{1}{3}$ – 2 $\frac{1}{2}$ III 1 – 2 IV 2 2/3 –1 V) (Fig. 5-II vs 5VII; Sup. Table 4).

Tadpoles and acoustics. Unknown

Distribution and natural history. Hylarana hellenae sp. nov. is currently only known from Sumatra, Jambi, Tapan, Kerinci Seblat National Park, 500–775 m a.s.l. (see Kurniati 2008). It was found along fast-moving streams in lowland primary rain forest, and breeds in slow-moving streams.

Discussion

The Hylarana signata complex, distributed across Sundaland (Borneo, Peninsular Malaysia, and Sumatra) and the Philippines, is structured into two principal clades consistent with earlier regional syntheses. Clade I contains the Philippine taxa (H. mangyanum, H. grandocula, H. moellendorffi, H. similis), together with the Bornean H. picturata and H. signata, and H. sundabarat from Peninsular Malaysia and southern Thailand (Brown & Guttman 2002, Chan et al. 2014, Arifin et al. 2018). Clade II contains the Sumatran endemics H. siberu, H. centropeninsularis, and H. fantastica, to which we add two Sumatran species described here, H. anantambanii sp. nov. and H. hellenae sp. nov. This dual structure reaffirms the phylogenetic integrity of the *signata* complex while demonstrating regional diversification within Our results also document H. Sumatra.

sundabarat widely across Sumatra, extending the picture presented by Chan et al. (2014; figures 1 & 3) and clarifying that H. signata and H. picturata remain Bornean endemics.

Mitochondrial phylogeny based on a 444-bp fragment of 16S resolves H. anantambanii sp. nov. and H. hellenae sp. nov. as strongly supported, reciprocally monophyletic lineages within Clade II, distinct from H. fantastica, H. siberu, and H. centropeninsularis. Pairwise divergence between the two new species is 4.81%, with deeper divergences to other Sumatran congeners (8.03–10.55%). values exceed commonly used thresholds for species-level differentiation in anurans (e.g., 2– 3% for 16S; Fouquet et al. 2007, Crawford et al. 2010, Lyra et al. 2017) and compare favourably with smaller interspecific distances reported elsewhere in the complex (e.g., 2.29% between H. grandocula and H. similis in the Philippines). Although the dataset was limited mitochondrial evidence, the strength of the phylogenetic signal, combined with consistent morphological distinctions, justifies recognition of both taxa as distinct species.

Morphometric ordination by PCA detects clustering that broadly tracks nominal taxa, with partial overlap typical of this group. The two new species are separable from close relatives by stable combinations of characters (e.g., humeralgland size and placement, dorsolateral stripe width and continuity, webbing formulae) together with mitochondrial distinctiveness, rather than by any single metric alone. This pattern aligns with previous studies showing shallow external differentiation but strong genetic partitioning across the H. signata complex (Brown & Guttman 2002, Chan et al. 2014, Arifin et al. 2018) and the influence of gene flow in shaping apparent cryptic diversity (Chan et al. 2020b). These findings emphasize morphology reliance on underestimates diversity amphibian in Sundaland.

Biogeographic patterns. Biogeographically, the present ranges are concordant with major Sumatran geological and ecological structures. Hylarana anantambanii sp. nov. is confirmed from Lampung and Bengkulu in the southwestern Barisan region, whereas H. hellenae sp. nov. occurs in Jambi (Kerinci Seblat National Park) in central-western Sumatra. Longrecognized tectono-sedimentary provinces and arches, including the South Sumatra Basin and Asahan Arch, are plausible semi-permeable

barriers to lowland and foothill amphibians and may have contributed to lineage isolation during the Middle Miocene to Pliocene (Pubellier & Morley 2014, Heidrick & Aulia 1993, Kurniati & Mujiono 2020). These geographic divisions correspond closely to faunal transition zones proposed for other vertebrate taxa, suggesting recurrent evolutionary isolation within Sumatra's orogenic corridors. Bengkulu's dissected hill systems correspond to its elevated endemism, Jambi harbours distinct amphibian assemblages relative to western and northern provinces (Kurniati & Mujiono 2020). Within this context, H. sundabarat is more widespread Sumatra than previously appreciated, occurring from Aceh to Bengkulu. Although our mapping indicates regional co-occurrence of H. sundabarat with H. anantambanii sp. nov., we did not document strict syntopy with H. hellenae sp. nov. at the type locality. Targeted surveys are needed to test for site-level sympatry. Future genomic analyses could evaluate whether contact zones exhibit hybridization or secondary gene flow.

Conservation implications. Both Н. anantambanii sp. nov. and H. hellenae sp. nov. are currently known from few localities, albeit within large protected areas (Bukit Barisan Selatan NP and Kerinci Seblat NP). Given limited samples and uncertain extent of occurrence, we recommend listing both as Data Deficient (DD) pending further population assessments. In contrast, H. sundabarat occupies a broad ecological and elevational range on Sumatra and the Peninsula Malaysia, warranting a preliminary listing inference of Least Concern (LC), subject to formal IUCN evaluation. The discovery of these new taxa reinforces the conservation value of Sumatra's remaining montane and submontane forests, which act as refugia for microendemic lineages. These conclusions align with established findings that primary forests are irreplaceable for tropical biodiversity (Gibson et al. 2011) and that protected landscapes in Indonesia experienced relatively lower deforestation rates in recent years (Gaveau et al. 2022). Sustained protection and targeted inventories in foothill and lower montane habitats remain essential for documenting true range limits, contact zones, and habitat associations.

Limitations and priorities. Our mitochondrial matrix is short by modern standards and cannot alone resolve the role of gene flow previously noted in this complex (Chan *et al.* 2020b). Future

integrative work should incorporate multilocus or genomic datasets, call structure analyses, larval morphology, and ecological niche modelling to species boundaries and population connectivity. Nonetheless, the congruence across phylogeny, morphometrics, external diagnoses, and geography provides a coherent basis for recognizing H. anantambanii sp. nov. and H. hellenae sp. nov. and for updating the Sumatran distribution of H. sundabarat. Together, these results refine the taxonomy of the H. signata complex in Sumatra and underscore the persistence of cryptic amphibian diversity within the forests of the Barisan mountain range. This underscores Sumatra's continued significance as a centre of herpetofaunal diversification within the Sunda Shelf.

Author contributions

All the authors contributed equally

Acknowledgments

We thank A.E. Herlambang, M.A. Fauzi, and A.D. Gonggoli for valuable insights; Mulyadi for assistance during the specimen examination; Rury Eprilurahman (Universitas Gadjah Mada, Indonesia), Koshiro Eto (Kitakyushu Museum of Natural History & Human History, Japan), and two anonymous reviewers for reviewing the manuscript.

Research permits

Ministry of Research and Technology of the Republic of Indonesia (RISTEK) and LIPI, which is now the National Research and Innovation Agency (BRIN) approved our fieldwork in Indonesia and provided export permits for specimen accessioning at UTA. The Forestry Department of Indonesia provided research permits for areas under its jurisdiction. Research in Indonesia was conducted under research permits 151/SIP/FRP/SM/V/2013 and 151A/SIP/FRP/SM/XII/2013 (ENS). ENS is grateful to S. Wahyono (RISTEK) for helping throughout the permit approval process.

Funding information

This research was funded by the Kemendiktisaintek RI (Government) under the master's thesis research scheme (No. 23251/IT3.D10/PT.01.03/P/B/2025) and the National Science Foundation grant (DEB-1146324). AATA is acknowledged for the Postdoctoral fellowship of the National Research and Innovation Agency (BRIN).

Supplemental data

https://doi.org/10.47605/tapro.v14i2.377

Literature Cited

- Arifin, U. (2024). Current knowledge of amphibian diversity in Sumatra and its conservation significance. *Oryx*, 58(4): 462–467.
- Arifin, U., G. Cahyadi, U. Smart, A. Jankowski & A. Haas (2018). A new species of the genus *Pulchrana* Dubois, 1992 (Amphibia: Ranidae) from Sumatra, Indonesia. *Raffles Bulletin of Zoology*, 66: 277–299.
- Boulenger, G.A. (1920). A monograph of the South Asian, Papuan, Melanesian & Australian frogs of the genus *Rana*. *Records of the Indian Museum*, 20: 1–226.
- Brown, R.M. & S.I. Guttman (2002). Phylogenetic systematics of the *Rana signata* complex of Philippine & Bornean stream frogs: reconsideration of Huxley's modification of Wallace's Line at the Oriental–Australian faunal zone interface. *Biological Journal of the Linnean Society*, 76(3): 393–461.
- Chan, K.O., R.M. Brown, K.K.P. Lim, N. Ahmad & L.L. Grismer (2014). A new species of frog (Amphibia: Anura: Ranidae) of the *Hylarana signata* complex from Peninsular Malaysia. *Herpetologica*, 70(2): 228–240.
- Chan, K.O., R.K. Abraham, L.L. Grismer & R.M. Brown (2020a). A systematic review of the *Pulchrana picturata* complex, with the description of a new species from Peninsular Malaysia, Sumatra & southern Thailand. *Raffles Bulletin of Zoology*, 68: 880–890.
- Chan, K.O., C.R. Hutter, P.L. Wood Jr., L.L. Grismer, I. Das & R.M. Brown (2020b). Gene flow creates a mirage of cryptic species in a Southeast Asian spotted stream frog complex. *Molecular Ecology*, 29(20): 3970–3987.
- Crawford, A.J., K.R. Lips & E. Bermingham (2010). Epidemic disease decimates amphibian abundance, species diversity & evolutionary history in the highlands of central Panama. *Proceedings of the National Academy of Sciences of the USA*, 107(31): 13777–13782.
- Fouquet, A., A. Gilles, M. Vences, C. Marty, M. Blanc & N.J. Gemmell (2007). Underestimation of species richness in Neotropical frogs revealed by mtDNA analyses. *PLoS ONE*, 2(10): e1109.
- Frost, D.R. (2025). Amphibian Species of the World. Version 6.2. www.amphibiansofthe.org Accessed on 4 Oct 2025.
- Gaveau, D.L.A., B. Locatelli, M.A. Salim, Husnayaen, T. Manurung, A. Descals *et al.* (2022). Slowing deforestation in Indonesia follows declining oil palm expansion & lower oil prices. *PLoS ONE*, 17(3): e0266178.

- Gibson, L., T.M. Lee, L.P. Koh, B.W. Brook, T.A. Gardner, J. Barlow *et al.* (2011). Primary forests are irreplaceable for sustaining tropical biodiversity. *Nature*, 478(7369): 378–381.
- Guayasamin, J.M., M.R. Bustamante, D. Almeida-Reinoso & W.C. Funk (2006). Glass frogs (Centrolenidae) of Yanayacu Biological Station, Ecuador, with the description of a new species & comments on centrolenid systematics. *Zoological Journal of the Linnean Society*, 147(4): 489–513.
- Günther, A. (1872). On the reptiles & amphibians of Borneo. *Proceedings of the Zoological Society of London*, 1872: 586–600.
- Hedges, S.B., R.A. Nussbaum & L.R. Maxson (1993). Caecilian phylogeny & biogeography inferred from mitochondrial DNA sequences of the 12S rRNA & 16S rRNA genes (Amphibia: Gymnophiona). Herpetological Monographs, 7: 64–76.
- Heidrick, T.L. & K. Aulia (1993). A structural & tectonic model of the Coastal Plains Block, Central Sumatra Basin, Indonesia. *Proceedings of the Indonesian Petroleum Association*, 22(1): 285–317.
- Kok, P.J.R. & M. Kalamandeen (2008). Introduction to the Taxonomy of the Amphibians of Kaieteur National Park, Guyana. ABC Taxa (Volume 5). Royal Belgian Institute of Natural Sciences, Brussels: 278 pp.
- Kurniati, H. (2008). Biodiversity & Natural History of Amphibians & Reptiles in Kerinci Seblat National Park, Sumatra, Indonesia. Research Center for Biology–LIPI, Cibinong: 100 pp.
- Kurniati, H. & N. Mujiono (2020). Distribusi geografi jenis-jenis kodok endemik Sumatra berdasarkan batas administratif provinsi & nilai penting wilayah konservasi. *Jurnal Biologi Indonesia*, 16(2): 183–194.
- Leong, T.M. & B.L. Lim (2004). *Rana siberu* Dring, McCarthy & Whitten, 1990 a first record for Peninsular Malaysia (Amphibia: Anura: Ranidae). *Raffles Bulletin of Zoology*, 52(1): 261–263.
- Lyra, M.L., C.F.B. Haddad & A.M.L. de Azeredo-Espin (2017). Meeting the challenge of DNA barcoding Neotropical amphibians: polymerase chain reaction optimization & new COI primers. *Molecular Ecology Resources*, 17(5): 966–980.

- Matsui, M. (1984). Morphometric variation analyses & revision of the Japanese toads (genus *Bufo*, Bufonidae). *Contributions from the Biological Laboratory, Kyoto University*, 26: 209–428.
- Mistar (2003). Panduan lapangan amfibi Kawasan Ekosistem Leuser. Gibbon Foundation, Jakarta & PILI-NGO Movement, Bogor: 111 pp.
- Okonechnikov, K., O. Golosova & M. Fursov; the UGENE team (2012). Unipro UGENE: a unified bioinformatics toolkit. *Bioinformatics*, 28(8): 1166–1167.
- Palumbi, S.R., A. Martin, S. Romano, W.O. McMillan, L. Stice & G. Grabowski (1991). *The Simple Fool's Guide to PCR, Version 2.0*. Kewalo Marine Laboratory, University of Hawaii, Honolulu.
- Portik, D.M., J.W. Streicher & J.J. Wiens (2023). Frog phylogeny: a time-calibrated, species-level tree based on hundreds of loci & 5,242 species. *Molecular Phylogenetics & Evolution*, 188: 107907.
- Pubellier, M. & C.K. Morley (2014). The basins of Sundaland (SE Asia): evolution & boundary conditions. *Marine & Petroleum Geology*, 58: 555–578.
- R Core Team (2020). R: A language & environment for statistical computing. R Foundation for Statistical Computing, Vienna, Austria.
- Ronquist, F., M. Teslenko, P. van der Mark, D.L. Ayres, A. Darling, S. Höhna *et al.* (2012). MrBayes 3.2: efficient Bayesian phylogenetic inference & model choice across a large model space. *Systematic Biology*, 61(3): 539–542.
- Savage, J.M. & W.R. Heyer (1997). Digital webbing formulae for anurans: a refinement. *Herpetological Review*, 28(3): 131.
- Tanabe, A.S. (2007). Kakusan: a computer program to automate the selection of a nucleotide substitution model & the configuration of a mixed model on multilocus data. *Molecular Ecology Notes*, 7(6): 962–964.
- Zainudin, R. & S.N. Sazali (2012). A morphometric analysis of *Hylarana signata* group (previously known as *Rana signata* & *Rana picturata*) of Malaysia. *International Journal of Modern Physics: Conference Series*, 9: 199–208.

Appendix: Other Specimens Examined

- *Hylarana anantambanii* sp. nov.: MZB.Amph 3481, one adult male from Kubu Perahu, Bukit Barisan Selatan National Park, Lampung; UTA A 62444, one adult male from Kubu Perahu, Lampung Barat, Lampung; MZB.Amph 4065, 4066, 22790, three adult males from Air Sumur Melintang, South Bengkulu.
- H. centropeninsularis: MZB.Amph 28764, one adult male from Sarolangung District, Jambi; MZB.Amph 28765-28767, three adult males from HMHSOG, Hutan Harapan, Jambi; MUN 01061, MUN 011075, MUN 01076
- H. fantastica: MZB. Amph 23861, 23869, and 23862, two adult male and female collected from Sibolangit Boy Scout Camp, Bandar Baru, Sibolangit, Deli Serdang, North Sumatra; MZB.Amph 26062-26063, an adult and a female collected from Gunung Batee Meucica, Aceh Besar, Aceh; MZB.Amph 26064, an adult male collected near the road from Bireun to Takengon, Bener Merah, Aceh; MZB.Amph 13231, an adult male collected from Aek Bongbongan, Huristak, Padang Lawas, North Sumatra; MZB.Amph 13233-13236, four adult males collected from Lubuk Pining, Padang Lawas, North Sumatra; MZB.Amph 13237-13242, six adult males collected from Air Sira, North Sumatra; MZB.Amph 13243, 13244, 13245, 13246, two adult females and two adult males, collected from Bandar Baru, Sibolangit, Deli Serdang, North Sumatra;
- H. hellenae sp. nov.: MZB.Amph 14791-14794, four adult males collected from Kerinci Seblat National Park, West Sumatra.
- H. picturata: MZB.Amph 5926, 5927, 6124, 6044, 6059, three adult female and two adult male collected from South Kalimantan, Borneo; MZB.Amph 6759, 7224, an adult male and an adult female collected from Bentuang Karimun National Park, West Kalimantan, Borneo; MZB.Amph 7735, 7742, 7748: three adult males collected from Temalang, East Kalimantan, Borneo; 8828, 8841, 8880, 8832, 8864, 8865, 8867: three adult males and four adult females collected from Bulungan, North Kalimantan, Borneo; MZB.Amph 10712, an adult male collected from North Barito, Central Kalimantan, Borneo; MZB.Amph 15448, an adult female collected from Binusan, West Nunukan, North Kalimantan, Borneo; MZB.Amph 25128, an adult female collected from Emil Baru, South Kalimantan, Borneo; MZB.Amph 25721, 25722, two adult males collected from Gunung Lumut, East Kalimantan, Borneo.
- H. siberu: MZB.Amph 9377-9379, 10676, 10677, five adult males collected from Siberut Island, West Sumatra.
- H. signata: MZB.Amph 3162, an adult female collected from Kayan Mentarang National Park, Bulungan, North Kalimantan, Borneo; MZB.Amph 6262, 6267, 6266, 6268, 6270, two adult female and three adult male collected from Maruwai, East Kalimantan, Borneo; MZB.Amph 7218, an adult male collected from Bentuang Karimun National Park, West Kalimantan, Borneo; MZB.Amph 15452, an adult female collected from Nunukan, North Kalimantan, Borneo; MZB.Amph 15599, 15608, 15609: two adult males and an adult female collected from Kutai, East Kalimantan, Borneo; MZB.Amph 24502, 24504, 24505, 24516, 24518, an adult female and four adult males collected from Kayan Mentarang National Park, Malinau, North Kalimantan, Borneo; MZB.Amph 15614, 15615, two adult females collected from Tahap Ritan, Tabang, Kutai, East Kalimantan.